

Accepted Manuscript

Hexagonal boron nitride catalyst in a fixed-bed reactor for exothermic propane oxidation dehydrogenation

Jinshu Tian, Jinhan Lin, Mingliang Xu, Shaolong Wan, Jingdong Lin, Yong Wang

PII: S0009-2509(18)30235-5
DOI: <https://doi.org/10.1016/j.ces.2018.04.029>
Reference: CES 14161

To appear in: *Chemical Engineering Science*

Received Date: 3 January 2018
Revised Date: 9 April 2018
Accepted Date: 14 April 2018

Please cite this article as: J. Tian, J. Lin, M. Xu, S. Wan, J. Lin, Y. Wang, Hexagonal boron nitride catalyst in a fixed-bed reactor for exothermic propane oxidation dehydrogenation, *Chemical Engineering Science* (2018), doi: <https://doi.org/10.1016/j.ces.2018.04.029>

This is a PDF file of an unedited manuscript that has been accepted for publication. As a service to our customers we are providing this early version of the manuscript. The manuscript will undergo copyediting, typesetting, and review of the resulting proof before it is published in its final form. Please note that during the production process errors may be discovered which could affect the content, and all legal disclaimers that apply to the journal pertain.



Hexagonal boron nitride catalyst in a fixed-bed reactor for exothermic propane oxidation dehydrogenation

Jinshu Tian^a, Jinhan Lin^a, Mingliang Xu^a, Shaolong Wan^a, Jingdong Lin^{a,*} and Yong Wang^{a,b,c,*}

^a Department of Chemistry, College of Chemistry and Chemical Engineering, National Engineering Laboratory for Green Chemical Productions of Alcohols-Ethers-Esters, Collaborative Innovation Center of Chemistry for Energy Materials, Xiamen University, Xiamen 361005, China

^b Voiland School of Chemical Engineering and Bioengineering, Washington State University, Pullman, Washington 99164, United States

^c Institute of Interfacial Catalysis, Pacific Northwest National Laboratory, 902 Battelle Blvd., Richland, WA 99352, United States

Corresponding author :

Yong Wang (yong.wang@pnnl.gov)

Jingdong Lin (jdlin@xmu.edu.cn)

Abstract

Hexagonal boron nitride (h-BN) with high thermal conductivity is potentially an effective catalyst for highly exothermic propane oxidative dehydrogenation (ODH) reaction. Here, we report our experimental and theoretic studies of such a catalyst for propane ODH in a fixed-bed reactor. Based on the computational fluid dynamics calculation (CFD) results, the catalyst bed temperature increases by less than 1 °C in the h-BN catalyst bed which is much smaller than that (8 °C) in the VO_x/γ-Al₂O₃ catalyst bed at a similar propane conversion (25%) using a micro-tubular reactor with

a diameter of 6 mm. Even in an industrially relevant reactor with an internal diameter of 60 mm, a uniform temperature profile can still be maintained using the h-BN catalyst bed due to its excellent thermal conductivity as opposed to a temperature gradient of 47 °C in the VO_x/γ-Al₂O₃ catalyst bed. The results reported here provide useful information for potential application of h-BN catalyst in propane ODH.

Keywords: propane ODH; h-BN; CFD simulation; temperature profile; heat transfer

1 Introduction

Non-oxidative propane dehydrogenation process has been extensively practiced in the chemical industry^{1, 2}. However, this reaction is limited by thermodynamic equilibrium and is favored at high temperature due to its endothermic nature³. Propane oxidative dehydrogenation (ODH) reaction, on the other hand, offers remarkable advantages, including no thermodynamic constraint, alleviating the coking of catalysts and readily providing heat owing to its exothermic nature^{4, 5}. However, the hotspots are unavoidably present in the catalyst bed due to the highly exothermic nature of propane ODH, which can significantly accelerate the undesired over-oxidation of propene, leading to decreased propene selectivity and catalyst deactivation^{6, 7}. Therefore, it is highly desired to efficiently remove the reaction heat in ODH of propane⁸. The heat of reaction in the ODH of propane and associated reactions is shown as follows:



To prevent the formation of hotspots in the catalyst bed, efforts have been made by

either diluting the feed with an inert gas or catalyst bed with thermally conducting materials. In addition, microchannel reactors^{6,9,10}, structured catalysts (metal foam or fiber) etc.¹¹⁻¹³, and fluidized-bed reactor^{14, 15} have also been attempted. Thermal conductivity of the catalysts is a key to removing the heat of the exothermic ODH reaction. Unfortunately, traditional refractory metal oxide-supported catalysts, such as VO_x/γ-Al₂O₃, have poor thermal conductivity (less than 0.5 W/K m), which inevitably causes the hotspots in the catalyst bed¹⁶, resulting in undesired over-oxidation of propene to CO_x (CO and CO₂)¹⁷ and catalyst deactivation.

Hexagonal boron nitride (h-BN), a highly promising material with its unique physicochemical properties^{18,19}, especially high thermal conductivity (33 W/K m)^{20,21}, has been recently reported with unique and hitherto unanticipated catalytic performances for ODH reaction^{22, 23}. For example, Hermans's group reported that h-BN exhibits high selectivity to propylene (79%) and ethylene (12%) at 14% propane conversion²³. Besides, Lu's group also found that the hydroxylated edge of h-BN can efficiently catalyze propane ODH to propene with a superior selectivity (80.2%) but with only negligible CO₂ formation (0.5%) at a given propane conversion of 20.6%²². Based on the above the results, h-BN is expected to effectively suppress the over-oxidation of propene to CO_x in the ODH reactions, which is a key benefit for ODH of alkanes to olefins. To evaluate the potential application of h-BN in a fixed-bed reactor for industrial ODH process, the heat transfer and the temperature profile in the fixed-bed reactor using h-BN as catalyst were studied in this work, which is crucial to the commercial application of h-BN²⁴.

In this article, the temperature profiles in the h-BN catalyst bed for propane ODH was studied using the computational fluid dynamics calculation (CFD), which shows visual temperature profile in the catalyst bed^{11, 25}. The temperature profile was simulated along the axis and radial directions in the h-BN catalyst bed for propane ODH. A comparison was also made with using VO_x/γ-Al₂O₃ catalyst in a

micro-tubular reactor with an inner diameter of 6 mm. An industrial-scale fixed-bed reactor with an inner diameter of 60 mm was further simulated and the results generated can offer useful information for the potential commercialization of propane ODH process using h-BN as a catalyst in a fixed-bed reactor.

2 Experimental Section

2.1 Preparation of the catalysts

h-BN was commercially obtained from Qinhuangdao Eno High-Tech Material Development CO., LTD with the purity >99%, which is named as h-BN-C. The sample was used as provided without further chemical or thermal treatment. The h-BN-C catalyst before the reaction is named as h-BN-C fresh and the h-BN-C after the reaction is named as h-BN-C spent.

As a comparison, 5wt% VO_x/γ-Al₂O₃ catalyst was prepared by wet impregnation⁸. 1 g γ-Al₂O₃ support was impregnated with 5.7 mL 0.1 M NH₄VO₃ solution and the resultant slurry was stirred at room temperature for 12 h. After the impregnation, the catalyst was dried at 90 °C overnight and then calcined at 600 °C for 4 h. 5wt% VO_x/γ-Al₂O₃ was denoted as VO_x/γ-Al₂O₃.

2.2 Characterizations

X-ray powder diffraction (XRD) patterns were recorded on a Rigaku Ultima IV diffractometer (Rigaku, Japan). Cu K_α radiation (40 kV and 30 mA) was used as the X-ray source. For each sample, Bragg's angles (2θ) between 10° and 60° were scanned at a rate of 10 °/min. Specific surface areas of catalysts were measured by the Brunauer-Emmett-Teller (BET) method, using a Micromeritics Tristar 3020 surface area and porosimetry analyzer. Prior to the measurement, all samples were degassed at 150 °C for 6 h. Thermal gravimetric analyzer (TGA; TG 209F1 Netzsch Germany)

was used to investigate the carbon deposition of the spent catalysts. The samples were preheated at 80 °C and then heated to 970 °C at a rate of 10 °C/min in air (20 mL/min). Fourier transform infrared (FT-IR) spectra were obtained on a Nicolet 6700 spectrometer (Thermo Fischer Scientific). The FT-IR spectra of the samples were recorded in the range of 650-4000 cm⁻¹.

2.3 Catalytic test

The VO_x/γ-Al₂O₃ and h-BN-C (80-100 mesh) were tested without dilution to provide a direct comparison with the CFD results. Propane (99.9%) and a gas mixture (O₂:N₂:He = 1:8:1) were individually controlled using two mass flow controllers (Sevenstar) to provide a reaction gas feed of C₃H₈:O₂:N₂:He = 1:1:8:1. The reactor wall temperatures were set from 510 °C to 590 °C. The reaction products were analyzed by using a gas chromatography (GC2060, Shanghai Ruimin GC Instruments, Inc) which have a flame ionization detector (equipped with KB-Al₂O₃/Na₂SO₄ column) for hydrocarbon (C_xH_y) analysis and a thermal conductivity detector (equipped with TDX-01 column) for CO and CO₂ analysis. Control experiments with quartz show that there is negligible propane conversion without catalyst. In all tests, carbon mass balances exceed 95%. The C₃H₈ conversion (X) and product selectivity (S) were calculated using standard normalization method based on the carbon atom balance and defined as follows.

$$C_{\text{balance}} = \frac{(\sum N_i A_i f_i)_{in}}{(\sum N_i A_i f_i)_{out}}$$

$$X_{si}(\%) = \frac{\sum N_{pi} A_{pi} f_{pi} f_{si}}{\sum N_{si} A_{si} f_{si} + \sum N_{pi} A_{pi} f_{pi}} * 100$$

$$S_{pj}(\%) = \frac{N_{pj} A_{pj} f_{pj}}{\sum N_{pi} A_{pi} f_{pi}} * 100$$

$$GHSV(h^{-1}) = F_{\text{totl}} / V_{\text{cat}}$$

where s or p represents the reactant or product; i represent random gas in this reaction system; A_i and f_i are the chromatographic peak area and the calibration factor of species i .

V_{cat} = volume of catalyst loaded in reactor (mL)

F_{tot} = total flow of all inlet gas (mL/min)

N = the number of carbon atoms of component

GHSV = gas hourly space velocity (h^{-1})

For the calculation of activation energy (E_a), catalyst activities were measured in an isothermal, tubular, one-pass fixed-bed quartz reactor with 6 mm inner diameter at ambient pressure. During the experiment, we kept the total flow gas (standard conditions of temperature and pressure (STP), i.e., 293.15 K and 101.325 kPa) and GHSV constant at different reactor wall temperatures. The $\text{VO}_x/\gamma\text{-Al}_2\text{O}_3$ (80-100 mesh) catalyst was diluted with inert quartz particles (1:10) to eliminate the temperature gradients in the catalyst bed. The conversion of C_3H_8 was maintained at less than 10% for the calculation of E_a . A classic method was used for calculation of E_a , which is described in detail as below. First, the reaction rate equation of propane ODH was approximated as equation (4) where C_i is the concentration ($i = \text{C}_3\text{H}_8$ and O_2), m and n are the reaction order of C_3H_8 and O_2 , respectively. Second, the equation (5) can be obtained when taking logarithm of the equation (4). When the conversion of C_3H_8 was maintained at less than 10%, the concentration of C_3H_8 and O_2 can be approximately constant. Therefore, $\ln(-r_{\text{C}_3\text{H}_8})$ can be plotted as a function of $1/T$ and the slope is $-E_a/R$. Thus, we can obtain E_a , which equals to the slope multiplied by $-R$ (8.314 J/mol.K).

$$-r_{\text{C}_3\text{H}_8} = A \exp(-E_a/RT) [\text{C}_{\text{C}_3\text{H}_8}]^m [\text{C}_{\text{O}_2}]^n \quad (4)$$

$$\ln(-r_{\text{C}_3\text{H}_8}) = \ln A - E_a/RT + m \ln(\text{C}_3\text{H}_8) + n \ln(\text{O}_2) \quad (5)$$

2.4 Computational fluid dynamics calculation (CFD)

The numerical simulation of the temperature profile at steady state inside the fixed-bed quartz tubular reactor was performed using the commercial CFD code FLUENT 6.3.26. All the simulations were carried out in a three-dimensional physical system. The tubular reactor was divided into three parts and the wall temperature of middle part where the catalyst was loaded was set isothermal¹¹ (**Figure 1**). The catalyst bed in contact with the isothermal wall (Z_2) was initially set at a uniform temperature. In the simulation of propane ODH, 0.31 mL catalysts (voidage: 0.35; height of catalytic bed: 11 mm; tube diameter: 6 mm) were packed in the reactor. A gas mixture of propane ($3 \text{ mL(STP) min}^{-1}$) and $\text{O}_2/\text{N}_2/\text{He} = 1:8:1$ ($30 \text{ mL(STP) min}^{-1}$) was controlled by the calibrated mass flow controllers and fed into the reaction tube at a GHSV of $6,300 \text{ h}^{-1}$. For the simulation of the reactor with different tube diameters, we ensure the same ratio of bed height to tube diameter (11/6) with the constant GHSV ($6,300 \text{ h}^{-1}$). We assume that all the thermophysical properties of the materials (solids and gases) are functions of the local temperature and composition. The simulation results of C_3H_8 conversion with different temperatures were calculated through the difference between inlet and outlet of propane mole fraction. Equations for conservation of mass, heat and momentum can be found elsewhere²⁶⁻²⁸. The finite-rate volumetric reaction model was used to determine the reaction heat, and the reaction rate was approximated as:

$$r_{\text{C}_3\text{H}_8} = A \exp(-E_a/RT) [\text{C}_{\text{C}_3\text{H}_8}]^m [\text{C}_{\text{O}_2}]^n$$

where the C_i is the concentration ($i = \text{C}_3\text{H}_8$ and O_2), m and n are the reaction order of C_3H_8 and O_2 , respectively^{23, 29}, E_a represents activation energy, $r_{\text{C}_3\text{H}_8}$ is C_3H_8 consumption rate ($\text{mmol/g}_{\text{cat.s}}$) and A is pre-exponential factor.

Boundary conditions:

At $z = 0$, $T_f = T_{inlet}$;

From $z = Z_1$ to Z_3 : $T_{wall} = \text{set temperature}$

where z is the axis, T_f is the temperature of the fluid.

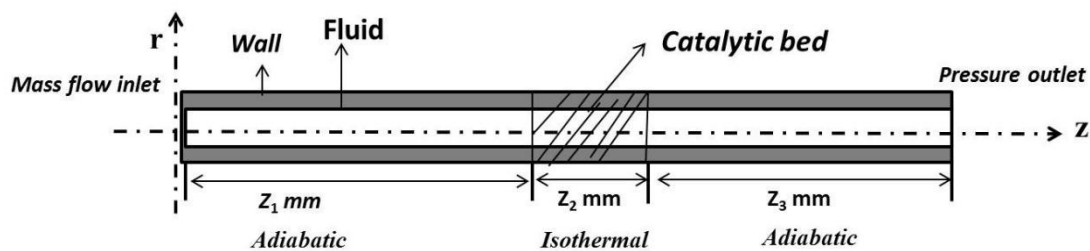


Figure 1 Schematic diagram of the system modeled by “FLUENT”

3 Results and Discussion

3.1 Catalytic performances of the catalysts

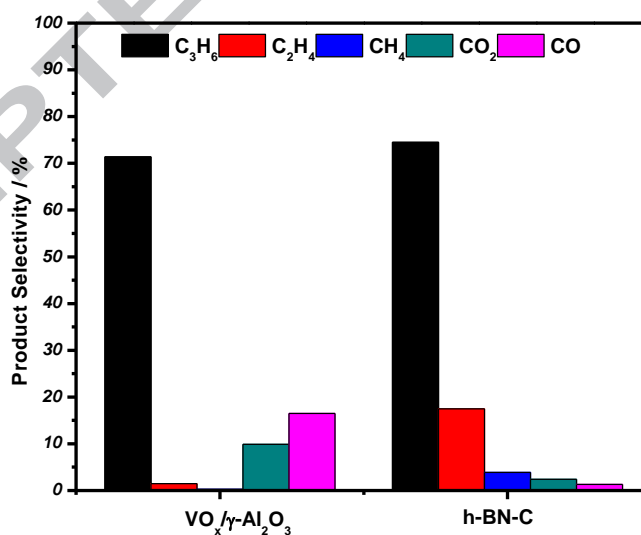
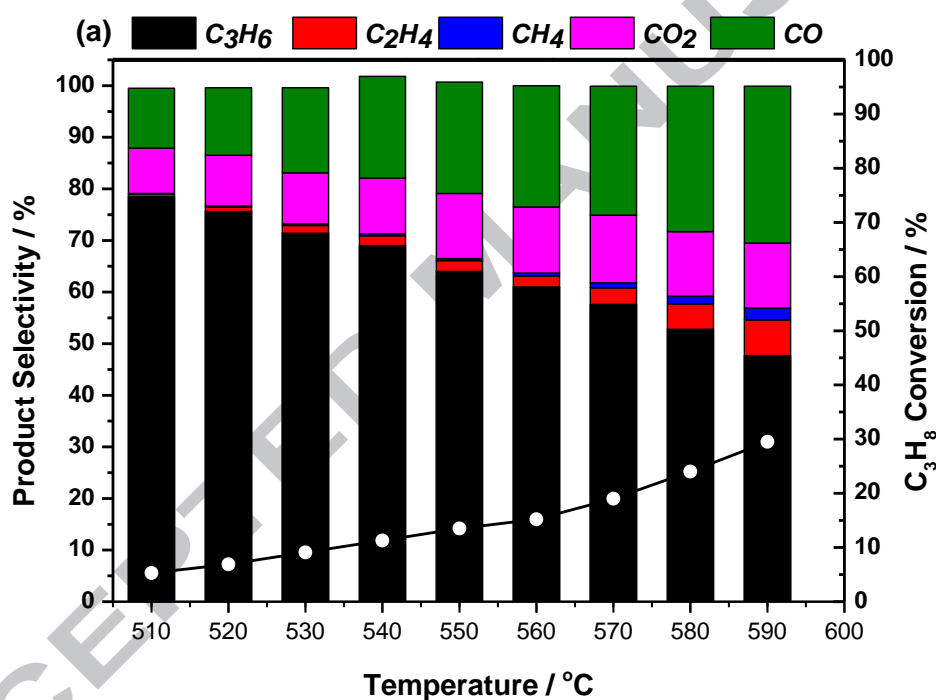


Figure 2 Product selectivities of propane ODH over VO_x/γ-Al₂O₃ (X = 9.1%) and h-BN-C (X = 8.3%) at 550 °C

Figure 2 shows the product selectivities over $\text{VO}_x/\gamma\text{-Al}_2\text{O}_3$ and h-BN-C catalysts for propane ODH at a similar propane conversion (9%). CO_x selectivity reached 26.4% on $\text{VO}_x/\gamma\text{-Al}_2\text{O}_3$ catalyst at 9.1% propane conversion. Compared to $\text{VO}_x/\gamma\text{-Al}_2\text{O}_3$ catalyst, h-BN-C exhibited a very low CO_x selectivity (3.7%) while achieving 93% olefin (propene and ethylene) selectivity at 8.3% propane conversion. Therefore, h-BN-C catalyst is much more selective for the propane ODH compared with the $\text{VO}_x/\gamma\text{-Al}_2\text{O}_3$ catalyst.



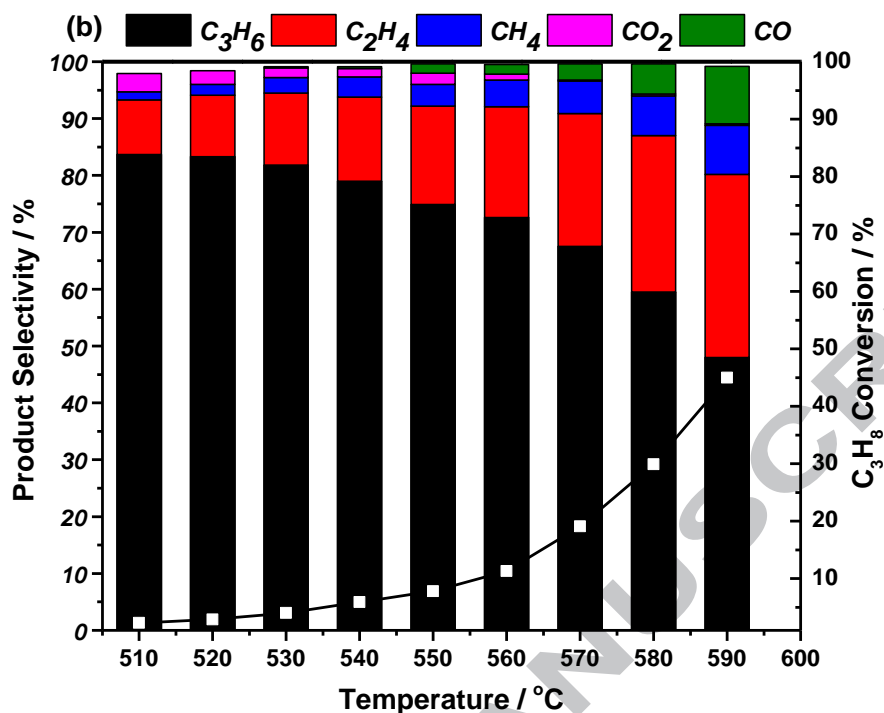


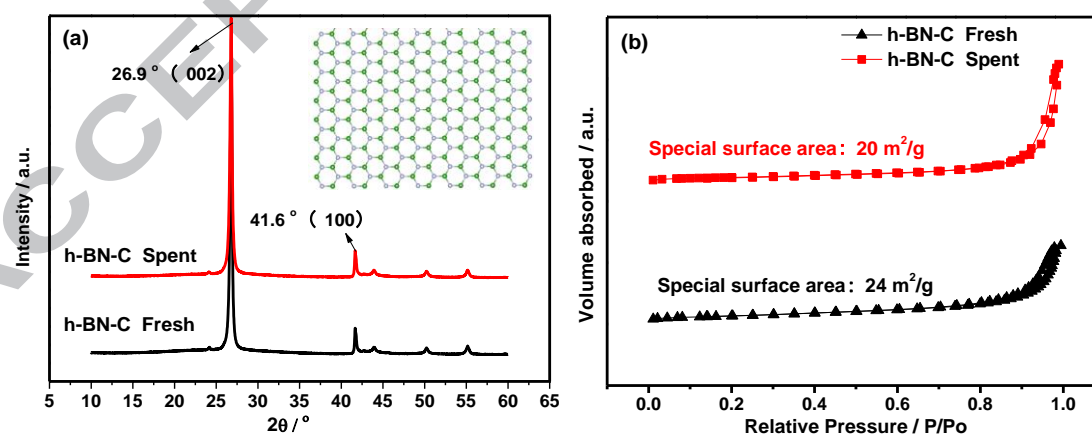
Figure 3 Influence of reaction temperature on the catalytic performances of propane ODH reaction over (a): VO_x/γ-Al₂O₃; (b): h-BN-C.

The reaction temperature is a crucial factor for propane ODH process. The influence of reaction temperature on propane conversion and product selectivities were thus studied in detail and results are shown in **Figure 3**. The conversion of propane continuously increased with increasing reaction temperature for both catalysts. However, as the reaction temperature increased from 510 °C to 590 °C, propene selectivity over the VO_x/γ-Al₂O₃ catalyst dropped dramatically from 78.5% to 47.7% with concurrent increase of CO_x selectivity (**Figure 3a**). It is typical for the VO_x/γ-Al₂O₃ catalyst to exhibit such a trade-off between propane conversion and propene selectivity³⁰. However, over the h-BN-C catalyst, olefin selectivity reached a maximum of 93.3% at 510 °C and still maintained at more than 80.0% with further increasing temperature even up to 590 °C at 45.0 % C₃H₈ conversion (**Figure 3b**). Over the VO_x/γ-Al₂O₃ catalyst, the main by-products are CO_x. Conversely, over the

h-BN-C catalyst, the main by-product is ethylene, a highly valuable olefin itself, rather than CO_x . Therefore, h-BN is potentially a promising catalyst for propane ODH reaction.

3.2 Characterizations of the fresh and spent h-BN-C catalysts

To better understand the structure stability of the h-BN-C catalyst, XRD, N_2 adsorption-desorption isotherms, FT-IR and TGA measurements were carried out to characterize the h-BN-C before and after the ODH reaction. As shown in **Figure 4 (a)**, the diffraction peaks at 2θ of 26.9° and 41.6° correspond to the (002) and (100) plane of h-BN crystalline phase (PDF#34-0421), respectively. All the h-BN-C samples exhibited similar diffraction patterns, indicating that crystalline structure of h-BN-C catalyst was maintained after the reaction. N_2 adsorption-desorption isotherms of the fresh and spent h-BN-C catalysts are displayed in **Figure 4 (b)**. The specific surface areas of the fresh and spent h-BN-C catalysts have the similar values of $24 \text{ m}^2/\text{g}$ and $20 \text{ m}^2/\text{g}$, respectively, suggesting the texture properties of h-BN-C catalysts being maintained after the reaction.



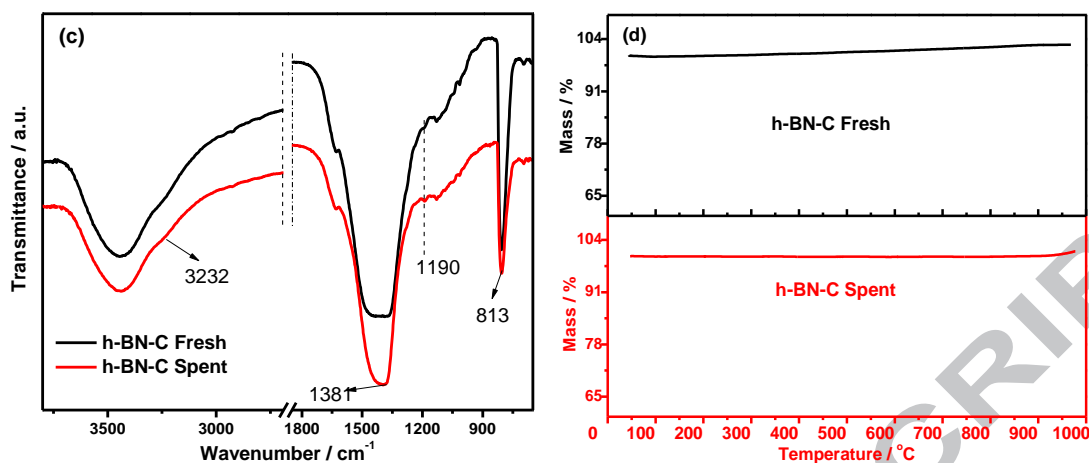


Figure 4 (a) XRD patterns of the fresh and spent h-BN-C catalysts with the structure model of h-BN; (b) N₂ adsorption–desorption isotherms of the fresh and spent h-BN-C catalysts; (c) FT-IR spectra of the fresh and spent h-BN-C catalysts; (d) TG curves of the fresh and spent h-BN-C catalysts in a flow of air.

FT-IR spectra of the fresh and spent h-BN-C catalysts were further obtained to determine the structures of the samples as shown in **Figure 4** (c). Based on the previous reports^{23,31}, the peaks at 1381 and 813 cm⁻¹ are assigned to the B-N stretching vibration and B-N-B bending vibration of h-BN, respectively. The two peaks are similar before and after the reaction, suggesting that the original B-N and B-N-B structures were maintained. However, the peaks at 3232 cm⁻¹ and 1190 cm⁻¹, which are assigned to OH stretching vibration and B-O stretching vibration, respectively, are simultaneously present after reaction, indicating that B-O and B-OH may be related to the active sites for the ODH reaction²². The amount of coke-deposition was measured by TGA in air at up to 970 °C. The results shown in **Figure 4** (d) suggest that the coke-deposition is not present over the spent h-BN-C catalyst.

Based on the characterizations mentioned above, the chemical structure of the h-BN-C catalyst is maintained after ODH reaction.

3.3 CFD simulations

The above results clearly indicate that the h-BN-C catalyst exhibits the superior performances for ODH reaction. However, the heat transfer and temperature profile in the catalyst bed are also vital to the highly exothermic propane ODH reaction and need to be studied.

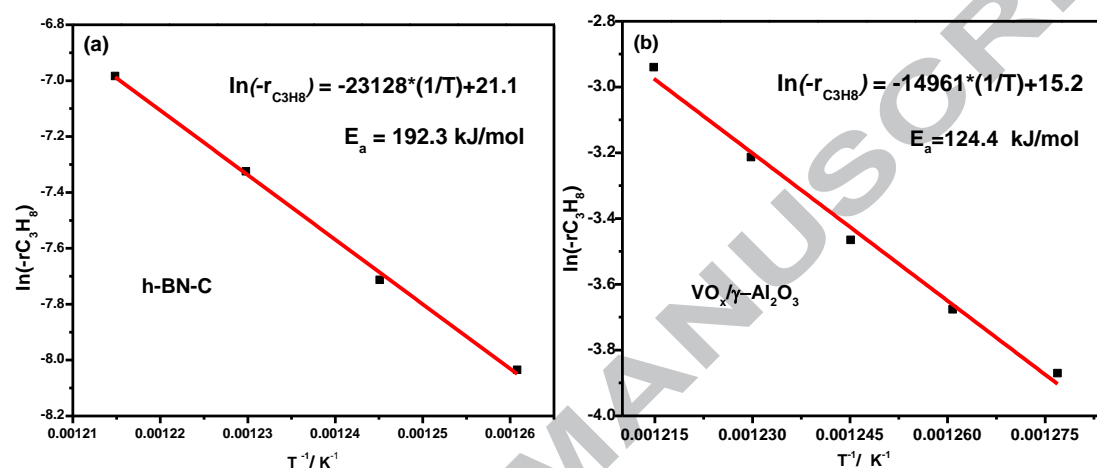


Figure 5 Logarithms of the reaction rate of propane ODH over different catalysts plotted as a function of $1/T$: (a) h-BN-C; (b) $VO_x/\gamma-Al_2O_3$.

The thermal conductivity of the catalysts is a key factor in removing the heat of the exothermic reaction¹¹. The h-BN-C catalyst has an excellent thermal conductivity of 33 W/m K, which is much higher than that of $VO_x/\gamma-Al_2O_3$ (0.5 W/m K), as listed in Table 1. The commercial CFD software ANSYS FLUENT 14.5 has been successfully used in other systems^{14, 16}. Here it was also used to simulate and compare the temperature profiles in both the h-BN-C catalyst and the $VO_x/\gamma-Al_2O_3$ catalyst bed. Propane ODH kinetic studies were carried out under the kinetic-limiting region over the h-BN-C and $VO_x/\gamma-Al_2O_3$ catalysts ($VO_x/\gamma-Al_2O_3$ was diluted using quartz with a catalyst: quartz weight (0.5 g) ratio of 1:10) in order to obtain the E_a . Based on the Arrhenius equation (**Figure 5**), an E_a of 192.3 kJ mol⁻¹ was obtained on h-BN-C

catalyst, which is higher than that on $\text{VO}_x/\gamma\text{-Al}_2\text{O}_3$ catalyst ($124.4 \text{ kJ mol}^{-1}$). These results were similar to those previously reported^{8, 22, 23}.

Table 1 Parameters (voidage and thermal conductivity) of the materials and E_a used in CFD calculation

Samples	Voidage	K_e (W/m K) ^a	E_a (kJ/mol)
h-BN-C	0.35	21.5	192.3
$\text{VO}_x/\gamma\text{-Al}_2\text{O}_3$	0.35	0.3	124.4

^a K_e is the effective thermal conductivity in the porous medium, which is calculated by $K_e = \epsilon K_{\text{fluid}} + (1-\epsilon)K_{\text{solid}}$, and ϵ is the voidage¹⁶.

The CFD simulation and approach were shown in **Figure 1**. To further confirm the reliability of the simulation results, we integrated the kinetic equation and the K_e into the CFD software, and made a comparison of the simulation conversions under the kinetic-limiting region over the two catalysts with the experimental results (**Figure 6 (a)** and **(c)**). Simulated results are very close to the experimental data, confirming the reliability of the simulations used in this study. The temperature profile in the catalyst bed was also simulated. The results shown in **Figure 6 (b)** and **(d)** confirms the uniform temperature in both cases for accurate kinetic data measurement.

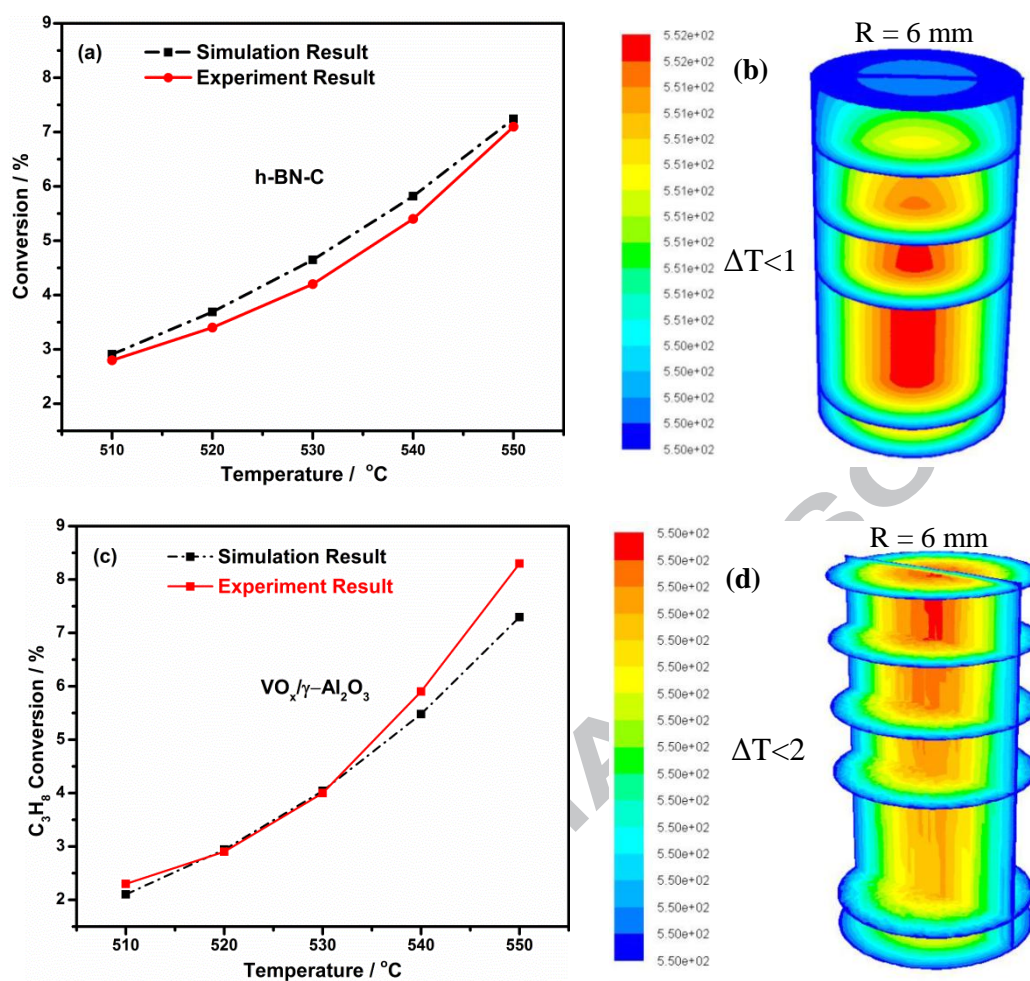


Figure 6 (a) C_3H_8 conversion from both the experimental and simulation results over h-BN-C catalyst without dilution; (b) 3D temperature profile of the fixed-bed reactor with h-BN-C catalyst (wall temperature at 550 $^{\circ}C$) over h-BN-C; (c) C_3H_8 conversion from both the experimental and simulation results over the $VO_x/\gamma-Al_2O_3$ catalyst (with 1:10 dilution using quartz); (d) 3D temperature profile of the fixed-bed reactor with $VO_x/\gamma-Al_2O_3$ catalyst. The unit of temperature is $^{\circ}C$.

CFD was thus used to analyze the temperature profile in the catalyst bed for propane ODH. The h-BN-C or $VO_x/\gamma-Al_2O_3$ catalyst was packed in the quartz tubular reactor (i.d. 6 mm) without dilution and subsequently simulated by CFD calculations using the above kinetic equation and the results are shown in **Figure 7**. The 3D

reaction rate profiles in catalyst bed over these two catalysts are also shown in **Figure 8**. For the highly exothermic propane ODH reaction, a higher temperature rise in the catalyst bed ($8\text{ }^{\circ}\text{C}$) is inevitable for the $\text{VO}_x/\gamma\text{-Al}_2\text{O}_3$ catalyst due to the low thermal conductivity of $\text{VO}_x/\gamma\text{-Al}_2\text{O}_3$ (0.5 W/m K)^{6, 7}. Whereas an equivalent amount of reaction heat is released from the catalyst bed at an equal propane conversion (25%) in both catalyst beds, less than $1\text{ }^{\circ}\text{C}$ hotspot temperature ($0.7\text{ }^{\circ}\text{C}$) is found in the h-BN-C catalyst bed, which is far less than that ($8\text{ }^{\circ}\text{C}$) in $\text{VO}_x/\gamma\text{-Al}_2\text{O}_3$ catalyst bed. This is attributed to the high thermal conductivity of h-BN, which enables more efficient removal of the reaction heat. Comparing the reaction rate of the two catalysts in **Figure 8 (a) and (b)**, it is found that the position of the most intensive reaction is different. The reaction rate is the highest at the inlet and gradually decreases along the fixed-bed reactor length over the h-BN-C catalyst, but for the $\text{VO}_x/\gamma\text{-Al}_2\text{O}_3$ catalyst, the highest reaction rate is near the inlet. It is not surprising that the position of the highest reaction rate is different over the two catalysts, because the reaction rate for propane ODH is the function of reactant concentration and reaction temperature. Over the $\text{VO}_x/\gamma\text{-Al}_2\text{O}_3$, the combination of hotspots in the middle of catalyst bed and high reactant concentration near the inlet led to highest reaction rate near the inlet while the catalyst bed temperature over the h-BN-C catalyst is relatively uniform and reaction rate is expected to be highest at the inlet where the reactant concentration is highest.

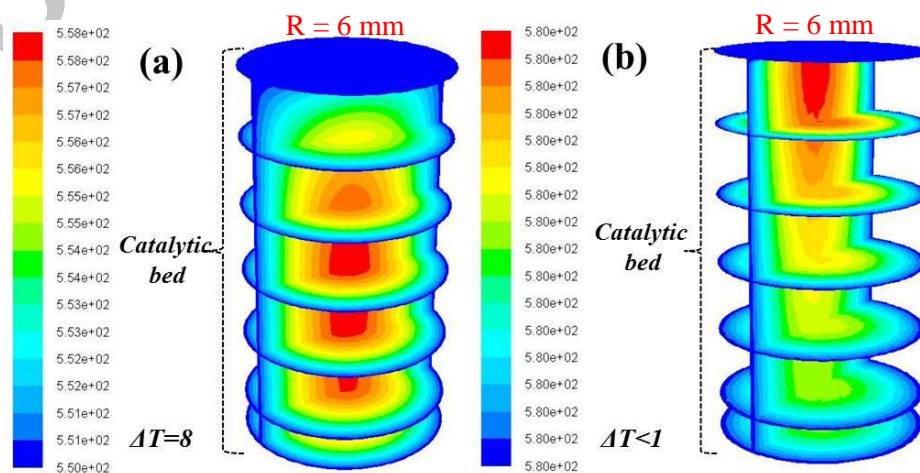


Figure 7 (a) 3D temperature profile of $\text{VO}_x/\gamma\text{-Al}_2\text{O}_3$ catalyst (without diluent) in the inner catalyst bed; (b) 3D temperature profile of h-BN-C catalyst in the inner catalyst bed. **Note:** the C_3H_8 conversions are 25% over the two catalysts with the same gas flow rate of 33 mL/min, which aimed to maintain the equal heat release. The unit of temperature is $^\circ\text{C}$.

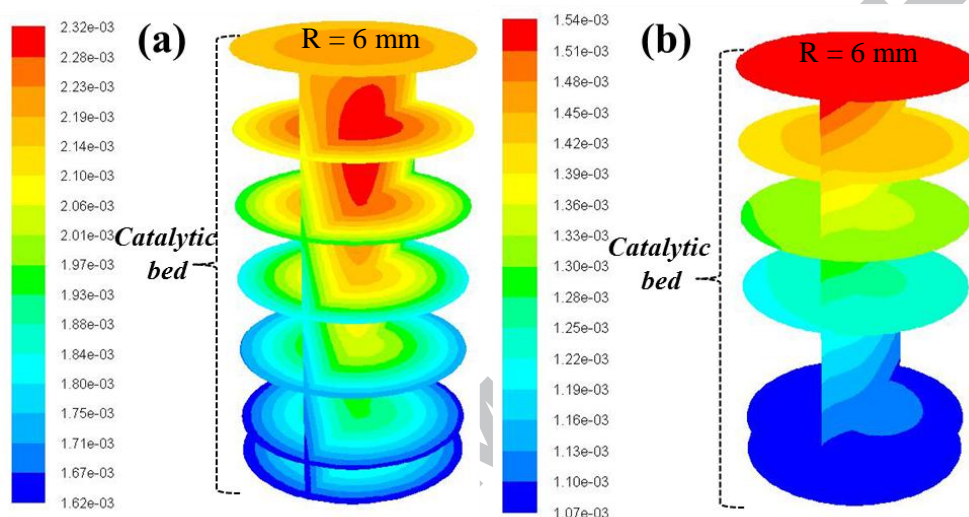
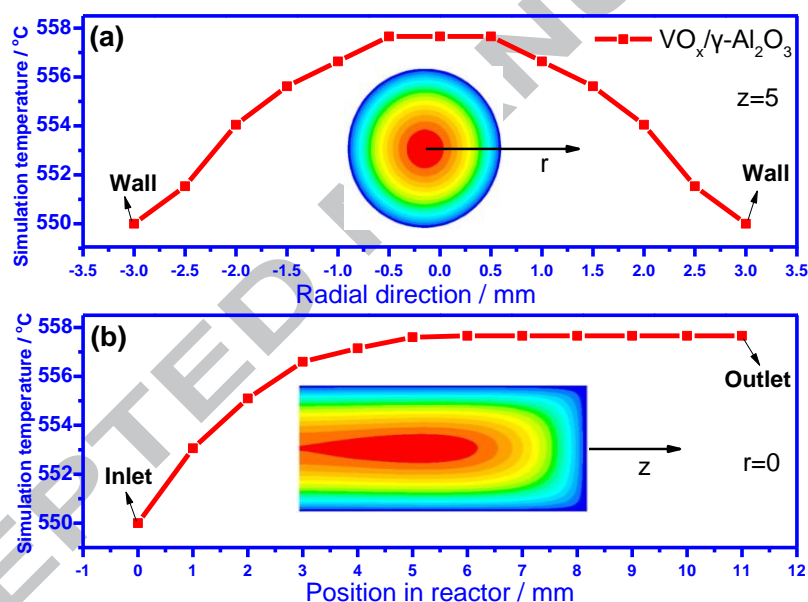


Figure 8 (a) 3D reaction rate profile of $\text{VO}_x/\gamma\text{-Al}_2\text{O}_3$ catalyst (without diluent) in the inner catalyst bed; (b) 3D reaction rate profile of h-BN-C catalyst in the inner catalyst bed. The unit of reaction rate is $\text{kmol/m}^3\cdot\text{s}$.

Figure 9 shows the temperature profiles along the radial direction and centerline axial direction of the catalyst bed, respectively. It is obvious that the temperature peaks symmetrically along the radial direction in **Figure 9** (a) over the $\text{VO}_x/\gamma\text{-Al}_2\text{O}_3$ catalyst but is relatively flat in **Figure 9** (c) over the h-BN-C catalyst. The different temperature profiles along the radial direction can be attributed to the different thermal conductivity of two catalysts. Due to the poorer thermal conductivity of the $\text{VO}_x/\gamma\text{-Al}_2\text{O}_3$ catalyst, a larger temperature gradient is present. The temperature profiles along centerline axial direction of catalytic bed over the two catalysts were

also simulated and the results are shown in **Figure 9 (b) and (d)**. Over the $\text{VO}_x/\gamma\text{-Al}_2\text{O}_3$ catalyst, temperature is similar to the wall temperature ($550\text{ }^\circ\text{C}$) near the inlet and gradually increases to about $558\text{ }^\circ\text{C}$ at the position of $z = 5\text{ mm}$ (distance from the inlet of the catalyst bed). However, there is almost no temperature gradient along the centerline axial direction of the h-BN-C catalyst bed. The above results demonstrate that the catalyst bed temperature is uniform in such a fixed-bed reactor configuration along both radial and centerline axial direction of the h-BN-C catalyst bed.



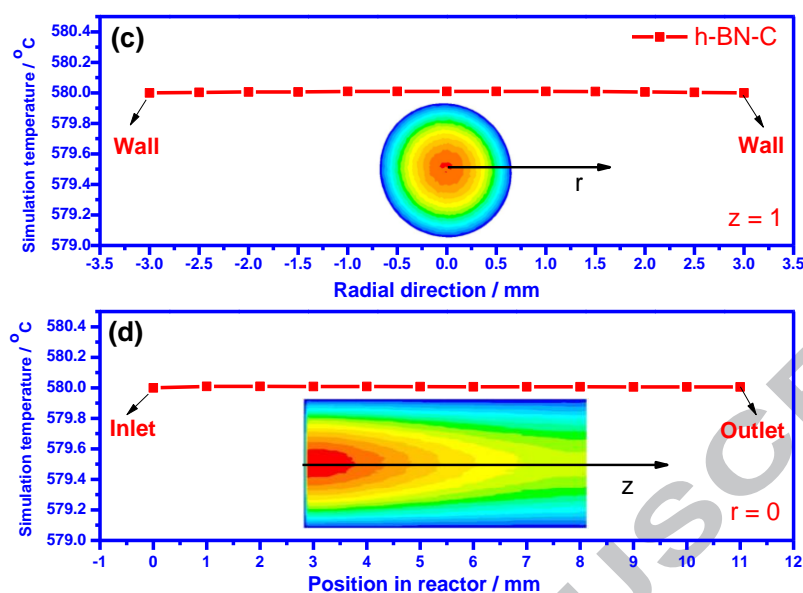


Figure 9 (a) The temperature profiles along the radial direction over $\text{VO}_x/\gamma\text{-Al}_2\text{O}_3$ catalyst bed at the position of $z = 5$ mm (distance from the inlet of the reactor); (b) The temperature profiles along centerline axial direction over $\text{VO}_x/\gamma\text{-Al}_2\text{O}_3$ catalyst bed at the position of $r = 0$ mm; (c) The temperature profiles along the radial direction over h-BN-C catalyst bed at $z = 1$ mm; (d) The temperature profiles along centerline axial direction over h-BN catalyst bed at $r = 0$ mm. **Note:** the illustrations represent temperature profile along the radial and centerline axis directions by CFD simulation.

When the temperature of reactor wall is further increased to 590 °C with a higher propane conversion of 45% over the h-BN-C catalyst, a uniform temperature profile can still be maintained as shown in **Figure 10 (a)**. In addition, the C_3H_8 mole fraction and reaction rate profiles shown in **Figure 10 (b) and (c)** are very similar over the h-BN-C catalyst. Therefore, reaction rate is just a function of propane concentration (not temperature since it's uniform), and therefore the temperature is isothermal even at a higher propane conversion (45%). The propane partial pressure will greatly affect the space time yield of propene due to the second-order dependence of propane in propane ODH over h-BN. Therefore, the isothermal condition maintained at a high propane

conversion (45%) in propane ODH over h-BN suggests that propane ODH can also be operated under an even higher propane partial pressure, leading to increased space time yield of propene which is desired for an industrial practice.

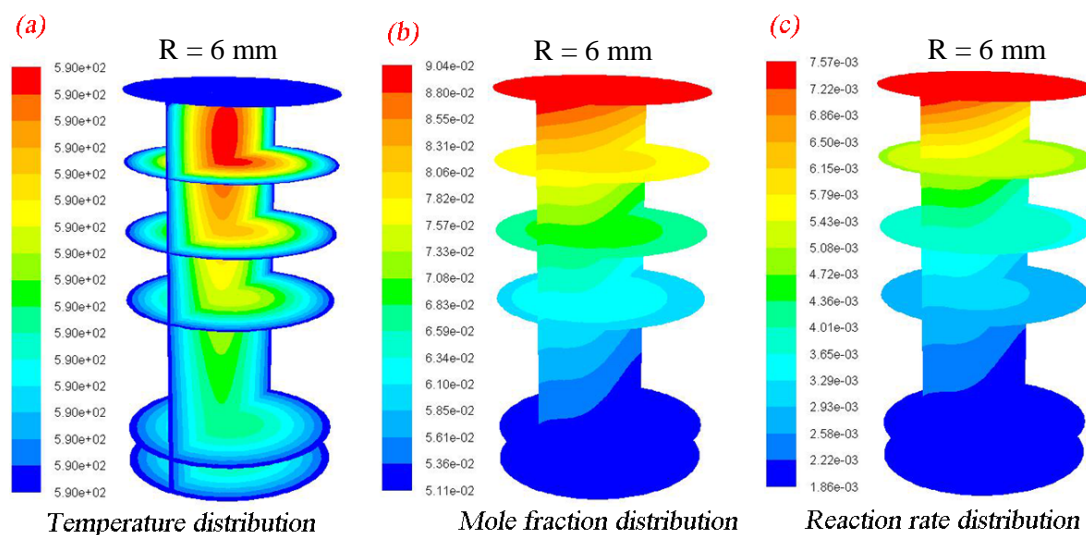


Figure 10 (a) 3D temperature profile of h-BN-C catalyst bed; (b) C_3H_8 mole fraction profile; (c) reaction rate profile. Note: The C_3H_8 conversion is 45% at the mixture feed gas flow rate of 33 mL/min at 590 °C. The unit of temperature and reaction rate is °C and $kmol/m^3 \cdot s$, respectively.

We further simulated the hotspots temperature in the catalyst bed over the two catalysts ranging from 520 °C to 590 °C and the results are shown in **Figure 11**. The hotspot is gradually developed over the $VO_x/\gamma-Al_2O_3$ catalyst bed as the wall temperature increases⁷. However, a uniform temperature profile can be maintained in h-BN-C catalyst bed even at high temperature which is attributed to the superior heat transfer ability. The results mentioned above indicate that the h-BN-C catalytic bed indeed can maintain a uniform temperature even at high conversion (45%) and 590 °C. However, it is inevitable to generate the hotspot (5 °C) in the $VO_x/\gamma-Al_2O_3$ catalyst

bed even at a lower temperature of 520 °C.

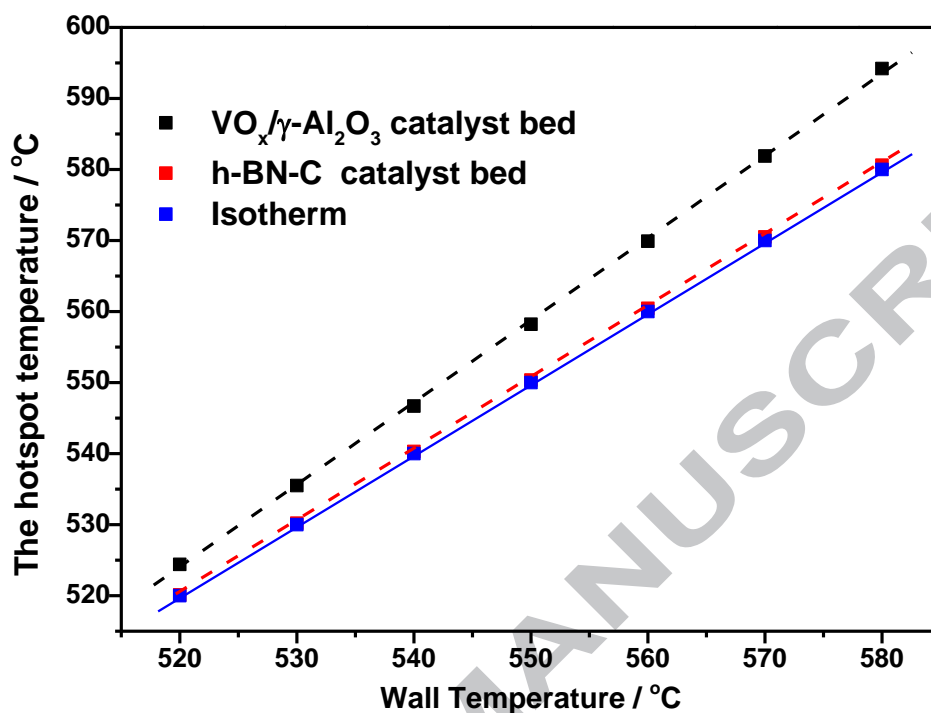


Figure 11 The simulated hotspot temperature plotted against wall temperature for both the VO_x/γ-Al₂O₃ and h-BN-C catalysts. GHSV: 6,300 h⁻¹ with different temperature.

In summary, high thermal conductivity of the h-BN-C catalyst can effectively dissipate the heat from a micro-tubular reactor with 6 mm diameter for propane ODH. The h-BN-C catalyst bed can be maintained under much more isothermal conditions compared to that using VO_x/γ-Al₂O₃ catalyst. Therefore, h-BN-C catalyst can potentially be used in a fixed-bed reactor for industrial practice of propane ODH^{22,23}.

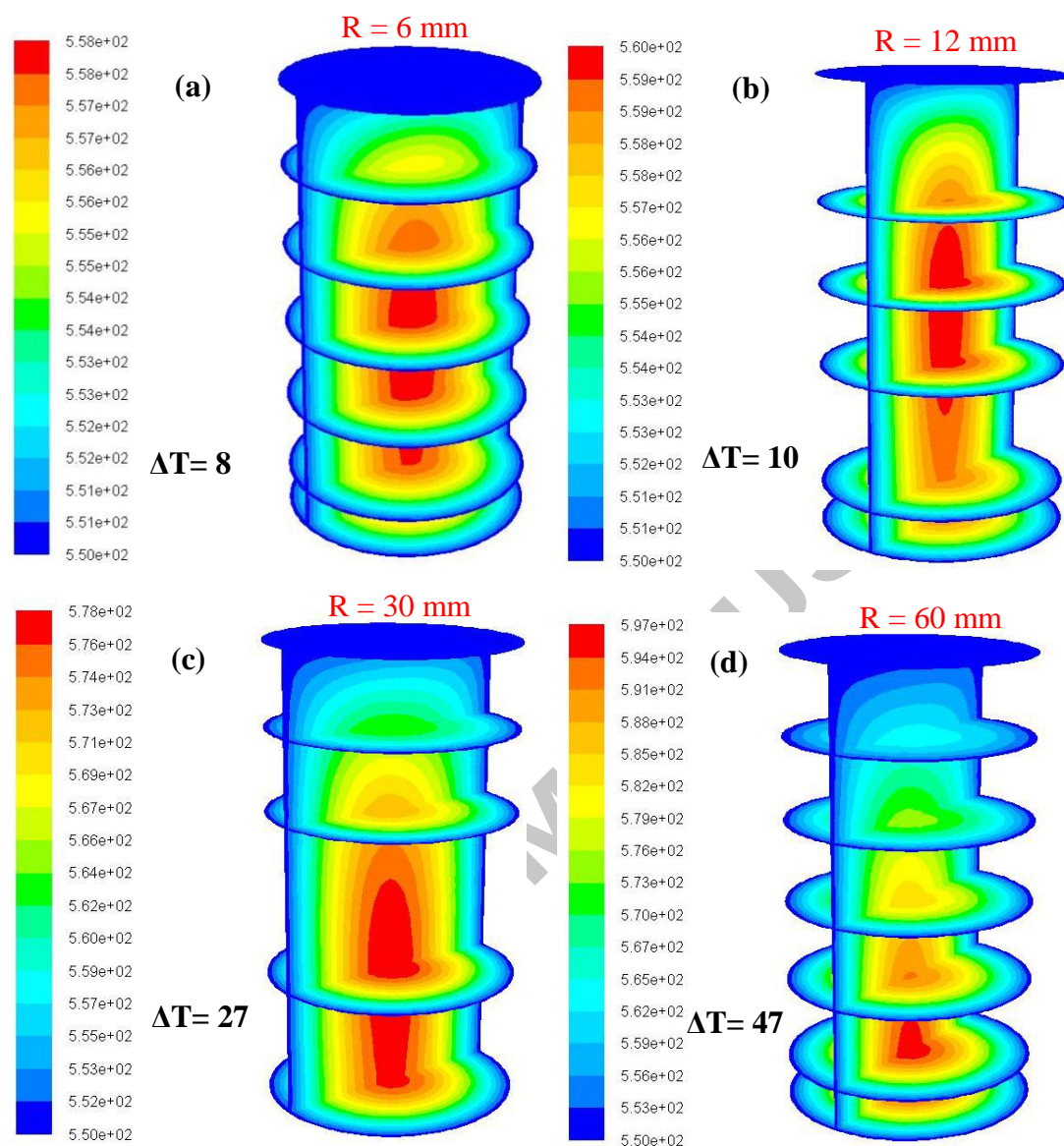


Figure 12 The temperature profile of $\text{VO}_x/\gamma\text{-Al}_2\text{O}_3$ catalyst bed with different reactor diameters (simulation condition: the same ratio of bed height and tube diameter with consistent GHSV of $6,300 \text{ h}^{-1}$ at $550 \text{ }^\circ\text{C}$): (a) 6 mm; (b) 12 mm; (c) 30 mm; (d) 60 mm.

The unit of temperature is $^\circ\text{C}$.

The inner tube diameter of a typical fixed-bed reactor for the industrial application is much larger than 6 mm. Therefore, the temperature profiles with different inner diameters (6-60 mm) of catalyst beds were further simulated. **Figure**

12 shows that the temperature gradient in the catalyst bed gradually increases with increasing inner diameter over the $\text{VO}_x/\gamma\text{-Al}_2\text{O}_3$ catalyst. When the inner diameter increases to 60 mm, the temperature gradient can reach up to 47 °C. As shown in **Figure 3 (a)**, the selectivity is very sensitive to the reaction temperature over the $\text{VO}_x/\gamma\text{-Al}_2\text{O}_3$ catalyst. Therefore, a 47 °C temperature gradient generated in the catalyst bed will significantly decrease the olefin selectivity. A fluidized-bed reactor has to be considered in the industrial practice to solve this “hotspot” problem of the highly exothermic reaction^{14, 24, 32}. However, a fluidized-bed reactor is more difficult to operate than a fixed-bed reactor, and has additional requirement of catalyst physical properties such as attrition resistance. On the other hand, the temperature profile in the h-BN-C catalyst bed is fairly uniform in the fixed-bed reactor (1.5 °C temperature gradient) even with an inner diameter of 60 mm as shown in **Figure 13**. Compared with the $\text{VO}_x/\gamma\text{-Al}_2\text{O}_3$ catalyst in a fixed-bed reactor, a much lower temperature gradient (1.5 °C) in the h-BN-C catalyst bed vs that in the $\text{VO}_x/\gamma\text{-Al}_2\text{O}_3$ catalyst bed (47 °C) in a fixed-bed reactor of 60 mm diameter suggests that the h-BN-C catalyst can indeed be commercially practiced in a fixed-bed reactor without sacrificing the product selectivity.

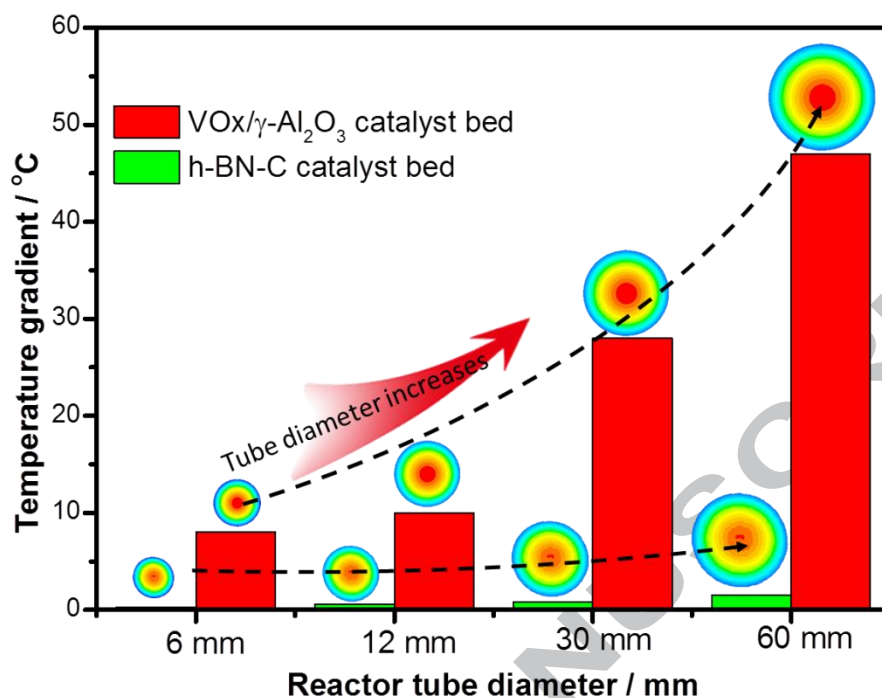


Figure 13 The temperature gradients of VO_x/γ-Al₂O₃ and h-BN-C catalyst beds with different tube diameters at the same GHSV

3 Conclusions

CFD simulation of a fixed-bed reactor was used to analyze the temperature profiles of the h-BN-C catalyst and VO_x/γ-Al₂O₃ catalysts for highly exothermic ODH process. The hotspot generated in h-BN-C catalyst bed (less than 1 °C) is much less than that (8 °C) of VO_x/γ-Al₂O₃ catalyst bed at a propane conversion of 25% in a micro-tubular reactor with a diameter of 6 mm. The high thermal conductivity of h-BN-C catalyst could maintain isothermal operation in such a micro-tubular reactor at even up to 590 °C with a higher propane conversion of 45%. However, a hotspot of > 5 °C temperature gradient is inevitable in the VO_x/γ-Al₂O₃ catalyst bed even at relatively low temperature of 520 °C. Using a fixed bed reactor with an inner diameter of up to 60 mm, which is close to the scale of an industrial practice, a uniform

temperature profile can be maintained over the h-BN-C catalyst (1.5 °C) as opposed to that in VO_x/γ-Al₂O₃ catalyst bed (47 °C). The significantly improved temperature control in the h-BN-C catalyst bed can lead to high selectivity towards olefin while minimizing CO_x formation. Therefore, the superior thermal conductivity the h-BN-C catalyst is attractive for its industrial practice of alkane ODH for olefin production in a fixed-bed reactor.

Acknowledgement

This work was supported by the National Natural Science Foundation of China (No. 21576227, No. 21673189, No. 91545114), the National Thousand Talents Program of P. R. of China, and the Fundamental Research Funds for the Central Universities (No. 20720160032).

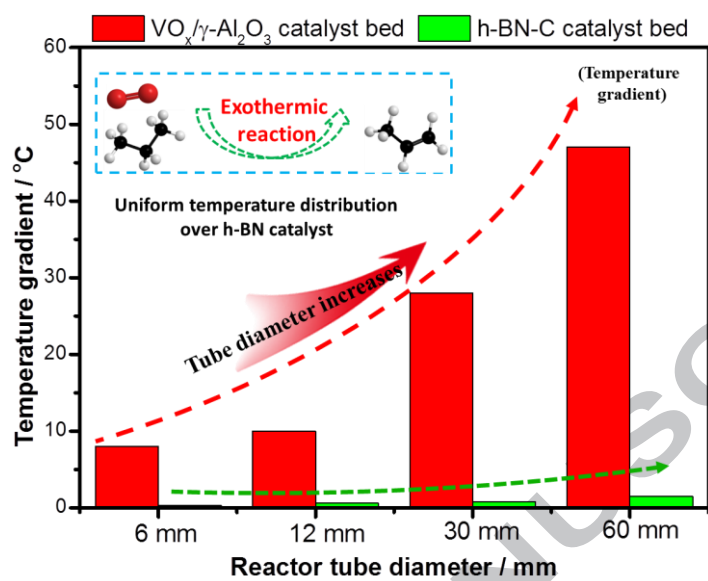
References

1. Otroshchenko, T.; Sokolov, S.; Stoyanova, M.; Kondratenko, V. A.; Rodemerck, U.; Linke, D.; Kondratenko, E. V., *Angew. Chem. Int. Ed. Engl.* **2015**, *54*, 15880-15883.
2. Liu, G.; Zhao, Z.; Wu, T.; Zeng, L.; Gong, J., *ACS Catal.* **2016**, *6*, 5207-5214.
3. Ayandiran, A. A.; Bakare, I. A.; Binous, H.; Alghamdi, S.; Razzak, S. A.; Hossain, M. M., *Catal. Sci. & Technol.* **2016**, *6*, 5154-5167.
4. Shylesh, S.; Singh, A., *J. Catal.* **2004**, *228*, 333-346.
5. Wu, J. C. S.; Lin, S., *Chem. Eng. J.* **2008**, *140*, 391-397.
6. Schwarz, O.; Duong, P. Q.; Schäfer, G.; Schomäcker, R., *Chem. Eng. J.* **2009**, *145*, 420-428.
7. Steinfeldt, N.; Buyevskaya, O. V.; Wolf, D.; Baerns, M., *Stud. Surf. Sci. Catal.* **2001**, *136*, 185-190.
8. Frank, B.; Dinse, A.; Ovsitser, O.; Kondratenko, E. V.; Schomäcker, R., *Appl. Catal. A* **2007**, *323*, 66-76.
9. Cao, C.; Hu, J.; Li, S.; Wilcox, W.; Wang, Y., *Catal. Today* **2009**, *140*, 149-156.
10. Baier, T.; Kolb, G., *Chem. Eng. Sci.* **2007**, *62*, 4602-4611.
11. Li, Y.; Zhang, Q.; Chai, R.; Zhao, G.; Liu, Y.; Lu, Y.; Cao, F., *AIChE J.* **2015**, *61*, 4323-4331.
12. Zhao, G.; Hu, H.; Deng, M.; Ling, M.; Lu, Y., *Green Chem.* **2011**, *13*, 55-58.
13. Palma, V.; Pisano, D.; Martino, M., *Chem. Eng. Sci.* **2018**, *178*, 1-11.
14. Lu, W. Z.; Teng, L. H.; Xiao, W. D., *Chem. Eng. Sci.* **2004**, *59*, 5455-5464.
15. Elbadawi, A. H.; Ba-Shammakh, M. S.; Al-Ghamdi, S.; Razzak, S. A.; Hossain, M. M.; de Lasa, H. I., *Chem. Eng. Sci.* **2016**, *145*, 59-70.
16. Li, Y.; Zhang, Q.; Chai, R.; Zhao, G.; Liu, Y.; Lu, Y., *ChemCatChem* **2015**, *7*, 1427-1431.
17. Löfberg, A.; Essakhi, A.; Paul, S.; Swesi, Y.; Zanota, M. L.; Meille, V.; Pitault, I.; Supiot, P.; Mutel, B.; Le Courtois, V.; Bordes-Richard, E., *Chem. Eng. J.* **2011**, *176-177*, 49-56.
18. Wu, P.; Zhu, W.; Dai, B.; Chao, Y.; Li, C.; Li, H.; Zhang, M.; Jiang, W.; Li, H., *Chem. Eng. J.* **2016**, *301*, 123-131.
19. Wu, P.; Zhu, W.; Chao, Y.; Zhang, J.; Zhang, P.; Zhu, H.; Li, C.; Chen, Z.; Li, H.; Dai, S., *Chem Commun (Camb)* **2016**, *52*, 144-147.
20. Li, M.; Zhu, W.; Zhang, P.; Chao, Y.; He, Q.; Yang, B.; Li, H.; Borisevich, A.; Dai, S., *Small* **2016**, *12*, 3535-3542.
21. Zhi, C., *Adv. Mater.* **2009**, *21*, 2889-2893.
22. Shi, L.; Wang, D.; Song, W.; Shao, D.; Zhang, W.; Lu, A., *ChemCatChem* **2017**, *9*, 1788-1793.
23. Grant, J. T.; Carrero, C. A.; Goeltl, F.; Venegas, J.; Mueller, P.; Burt, S. P.; Specht, S. E.; Mcdermott, W. P.; Chiericato, A.; Hermans, I., *Science* **2016**, *354*, 1570-1573.
24. Zaynali, Y.; Alaviamleshi, S. M., *Particul. Sci. Technol* **2017**, *35*, 667-673.
25. Tran, A.; Aguirre, A.; Durand, H.; Crose, M.; Christofides, P. D., *Chem. Eng. Sci.* **2017**, *171*, 576-598.
26. Zhao, G.; Li, Y.; Zhang, Q.; Deng, M.; Cao, F.; Lu, Y., *AIChE J.* **2014**, *60*, 1045-1053.
27. Chen, W.; Sheng, W.; Zhao, G.; Cao, F.; Xue, Q.; Chen, L.; Lu, Y., *Rsc Adv.* **2012**, *2*, 3651-3653.
28. Chen, W.; Sheng, W.; Cao, F.; Lu, Y., *Int. J. Hydrogen. Energ* **2012**, *37*, 18021-18030.
29. Chen, K.; Khodakov, A.; Yang, J.; Bell, A. T.; Iglesia, E., *J. Catal.* **1999**, *186*, 325-333.

-
30. Chen, K.; Bell, A. T.; Iglesia, E., *J. Phys. Chem. B* **2000**, *104*, 1292-1299.
 31. Hermans, I.; Venegas, J.; Grant, J. T.; McDermott, W. P.; Burt, S. P.; Micka, J.; Carrero, C. A., *ChemCatChem* **2017**, *9* 2118-2127
 32. Liu, B.; Ji, S., *J. Energy Chem.* **2013**, *22*, 740-746.

ACCEPTED MANUSCRIPT

Graphical abstract



Highlights:

1 h-BN is an effective catalyst for exothermic propane ODH in a fixed-bed reactor.

2 Temperature profile in catalyst bed for propane ODH was studied using CFD.

3 Nearly isothermal operation can be maintained using h-BN for industrial propane ODH.

ACCEPTED MANUSCRIPT